Gaussian Process Model Predictive Admittance Control for Compliant Tool-Environment Interaction

Wenxin Zhu[1,2], Wenyu Liang[2], Qianyuan Ren[1], Yan Wu[2]

***Abstract*— Humans demonstrate dexterous manipulation skills when holding different tools to physically interact with their environments, e.g., refined polishing of workpieces using tools with soft foams. During the polishing process, modeling tool-environment interaction is difficult because the robot may not have access to the physical properties of different compliant tools and environments (e.g., stiffness, shape, and friction). To address this challenge, a learning-based method has been employed to predict the contact model without explicitly knowing the intrinsic physical properties. Notably, the extrinsic contact is estimated using the intrinsic tactile sensing between the gripper and the tool in this work. Further, to ensure precise force control during the polishing process, a Gaussian process-based model predictive admittance control (GP-MPAC) scheme is developed with the estimated extrinsic contact. Finally, experiments have been conducted using a robot manipulator, and the results validate that the proposed method is effective while demonstrating its ability to handle the above-mentioned complexities.**

I. Introduction

Nowadays, there is a growing expectation for robots to perform human-like interaction tasks with objects/environments such as polishing/grinding [1], [2], ultrasound scanning [3], surgical operation [4], etc. These tasks require the robot to interact with the environment while holding tools, typically by contacting and moving across arbitrary surfaces with the desired contact force. In this work, we investigate the problem of controlling the compliant tool-environment interaction between the gripper-held tool and the environment, e.g., refined polishing of workpieces using tools with soft foams. It is worth noting that this work relies on intrinsic tactile sensing between the gripper and the tool to perceive the extrinsic tool-environment interaction.

Controlling the tool-environment interaction often relies on estimated models of physical tools or environments. These models serve the purpose of predicting the magnitude of forces exerted by the environment or identifying the characteristics of the environment in contact with the robot. Currently, the Kelvin-Boltzmann model and the Hunt-Crossley model [5], are widely adopted for capturing tool-environment interaction dynamics [6] due to their superior transient response estimation compared to other contact models [7]. As the robot moves along a trajectory, the parameters of the environmental model can be estimated online based on position and force information [8]. However, these model-based parameter identification methods often rely on precise nonlinear dynamic models and exhibit high computational complexity. To deal with dynamic modeling between different physical properties of compliant tools and environments (e.g., stiffness, shape, and friction), learning-based methods are crucial for accurately predicting the behavior of the contact model. Gaussian Process Regression (GPR) is a promising approach for this purpose due to its ability to model nonlinear relationships while providing uncertainty estimates. In the context of contact modeling, GPR can be employed to learn the mapping between input features, such as tool properties, environment characteristics, interaction parameters, and output contact forces.

The learning-based dynamics model demonstrates an online learning ability, enabling the robot to regulate its motion and forces when interacting with environments. Most current motion and force control schemes rely on impedance control, which generates compliant behavior for contact-rich tasks through a mass-spring-damper system [9]. However, with the classical impedance control, it is difficult to deal with multiple constraints at the same time, such as acceleration, speed, and force limits. As an advanced control method for controlling systems with multiple variables and constraints, model predictive control (MPC) has recently been combined with force/impedance control for interaction [10]–[14]. For example, in [14], a hierarchical strategy combining MPC and admittance control is proposed to address stability issues, where the MPC layer handles path planning and setpoint generation, while the admittance control layer ensures compliant behavior and stability during contact. However, in these studies, the choice of behavior focused on path point selection, which is not directly aligned with compliant behavior.

Further research is being conducted on methods to achieve prescribed compliant behavior through appropriate MPC formulations while satisfying practical robot constraints. The work presented in [15] is the first work to formulate the impedance control problem within the framework of MPC and validate it with a collaborative robot, namely, model predictive impedance control. Moreover, [16] presents a model predictive impedance model that uses impedance parameters as control inputs and designs the cost function to balance robot precision and compliance. Similarly, [17] combines MPC with impedance control

This work was supported by the National Natural Science Foundation, China (No.62088101) and the A*STAR C210812049.

[1]W. Zhu and Q. Ren are with the College of Control Science and Engineering, Zhejiang University, Hangzhou, China 310027 {wenxin_zhu, renqinyuan}@zju.edu.cn

[2]W. Zhu is also with the Institute for Infocomm Research, Agency for Science, Technology and Research, Singapore 138632.

[2]W. Liang and Y. Wu are with the Institute for Infocomm Research, Agency for Science, Technology and Research, Singapore 138632 {liang_wenyu, wuy}@i2r.a-star.edu.sg

to enable safe human-robot interaction. However, in most of these interaction tasks, force is not directly incorporated into the system state variables, which affects the rapid tracking effect of the force. The lack of dynamics modeling for external force in model predictive impedance control can be effectively addressed by introducing Gaussian Process Regression into the MPC framework. By combining the strengths of GPR for data-driven dynamics learning and MPC for constrained optimization, the GP-MPC approach can significantly enhance the adaptivity in complex and uncertain environments, enabling safe and efficient robot-environment interaction [18]–[21]. In [20], a GP-MPC is utilized to capture the residual dynamics, particularly the aerodynamic effects, acting on a quadrotor platform. Besides, in [21], the nominal dynamic models for real vehicles have been enhanced by the data-driven component using GP to complement the prediction model of the MPC. Nevertheless, there is still limited research on modeling the dynamics of tool-environment interaction using Gaussian process regression for model predictive impedance control.

This paper proposes a Gaussian process-based model predictive admittance control (GP-MPAC) scheme for polishing tasks with unknown contact dynamics. The main contributions are i) development of GPR mechanism for online adaptation of the nonlinear contact model to deal with the unknown tool-environment contact dynamics; ii) integration of admittance control with MPC, wherein the designed cost function is related to the desired impedance behavior such that multiple constraints can be effectively handled and optimal control can be achieved; iii) incorporation of contact force and state equations of the MPAC, enabling the consideration of contact force constraints such that the contact detachment or damage can be prevented.

The rest of this paper is organized as follows. Sections II and III introduce the problem statement and the system modeling, respectively. Next, the control design for GP-MPAC is detailed in Section IV. Section V presents the simulation and experiment results. Finally, the conclusion is drawn in Section IV.

II. Problem Statement

Consider a scenario where a robot manipulator is required to perform a tool-environment interaction task. In this task, the robot needs to move along a surface while applying a specific normal contact force. Fig. 1 illustrates a similar instance, such as a robotic polishing or grinding application. The tool-environment interaction dynamics can be modeled as nonlinear and time-invariant, expressed as

$$x_{k+1} = f(x_k, u_k), \tag{1}$$

with the state $x_k \in \mathbb{R}^n$ and control input $u_k \in \mathbb{R}^n$.

During the polishing process, the compliance of tools, high-frequency vibrations, and the inherent complexity of environmental conditions may induce unmodeled dynamics and external disturbances. Thus, the system model $f(x_k, u_k)$ is not known exactly which can be approximated by the combination of a nominal model and an unknown but bound disturbance

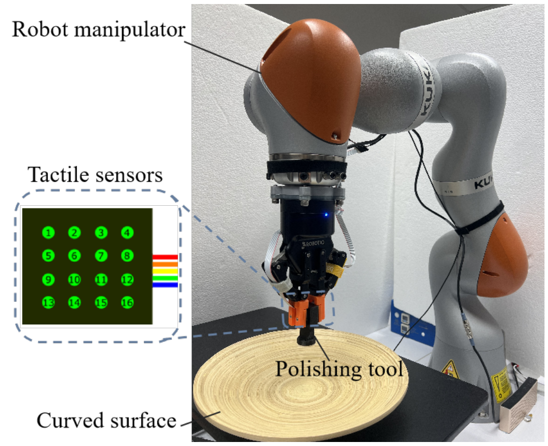

Fig. 1. Robotic polishing task.

model as shown below

$$x_{k+1} = f_{nom}(x_k, u_k) + B_d(g(z_k) + w), \tag{2}$$

where $f_{nom}(\cdot)$ refers to the discrete-time dynamics of the nominal model of the plant, $g(z_k)$ is the disturbance model, z_k refers to the regression features, B_d is the input matrix for disturbances, and the process noise w.

According to (2), a force controller needs to be designed for the robot to manipulate the tool on arbitrary shapes of surfaces with constraints. The discrete-time finite-horizon control problem of nonlinear MPC with terminal cost is given by

$$\begin{aligned} x^*_{0:N}, u^*_{0:N-1} = \underset{x_{0:N}, u_{0:N-1}}{\arg\min} & \sum_{k=0}^{N-1} f_o(x_k, u_k) + \phi(x_N) \\ \text{s.t. } & x_{k+1} = f_{\text{nom}}(x_k, u_k) + B_d(g(z_k) + w) \\ & x_0 = \bar{x} \\ & x_k \in \mathcal{X}(x_k) \\ & x_N \in \mathcal{X}_f \\ & u_k \in \mathcal{U}(x_k), \end{aligned} \tag{3}$$

where the cost function f_o and the final cost $\phi(x_N)$ are defined according to the force control problem and will be further described in Section IV.

III. System Modeling

A. Contact Model

In the robotic polishing process, the contact force is crucial because it directly influences the polishing effectiveness and quality. Significantly, a nonlinear function can be used to express the contact model between the tool and the unknown contacting objects/environments, which is shown as

$$F_e = \mathcal{F}(p, \dot{p}, t), \tag{4}$$

where $p \geq 0$ is the end-effector position of the tool, the environment equilibrium position is equal to zero, and F_e represents the intrinsic interaction force between the tool and the environment which can be estimated from the gripper-tool tactile sensing.

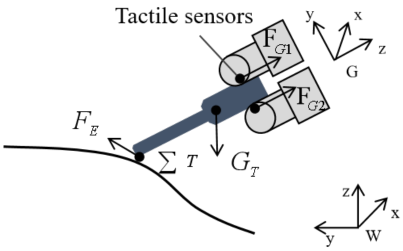

Fig. 2. Mechanics of robotic tool manipulation.

The time derivative of the contact model can be written as:

$$\dot{F}_e = \mathcal{F}'(p, \dot{p}, \ddot{p}, t). \tag{5}$$

B. Tool Dynamics

Robotic tool manipulation results in the formation of multiple contacts between different parts of the gripper, the tool, and the environment. Figure 2 illustrates a simplified contact diagram for robotic tool manipulation and defines the coordinate systems, where ΣW, ΣG, ΣT represent the coordinate systems of the world, the gripper, and the tool, respectively.

As the contacts among the gripper, the tool, and the environment are required to be maintained during the polishing task, the quasi-static equilibrium of the tool in the presence of these contacts can be described as

$$f\left(G_T, {}^W_G R F_{G1}, {}^W_G R F_{G2}, {}^W_T R F_E\right) = 0, \tag{6}$$

where G_T is the gravity of the tool, F_{G1} and F_{G2} are wrench from the two tactile sensors on the gripper to the tool, F_E is the wrench from the environment, ${}^W_G R$ is the rotation matrix from gripper coordinate system to world coordinate system, which can be calculated from the position feedback information of the manipulator, and ${}^T_W R$ is the rotation matrix from tool coordinate system to world coordinate system, which can be derived from ${}^T_W R = {}^G_W R {}^T_G R$.

As can be seen from (6), G_T, F_{G1}, and F_{G2} are measurable while ${}^W_G R$ and ${}^G_W R$ are known. Hence, the tool-environment extrinsic contact force indicated in F_E can be estimated based on (6).

C. Admittance Dynamics of the Manipulator

Considering the reference position $p_r(t)$, the reference force $F_r(t)$ in the Cartesian space and the contact force $F_e(t)$, the impedance control of a manipulator interacting with an unknown environment can be expressed by a control law as follows,

$$M_v(\ddot{p} - \ddot{p}_r) + D_v(\dot{p} - \dot{p}_r) + K_v(p - p_r) = K_f(F_e - F_r), \tag{7}$$

where p_r and F_r denote the reference position in the Cartesian space and the reference contract force, respectively. $M_v, D_v, K_v, K_f \in \mathbb{R}^{n \times n}$ are the desired inertia, damping, stiffness and force matrices for the admittance control.

The position and force tracking errors can be defined as $\xi_p(t) = p(t) - p_r(t)$ and $\xi_f(t) = F_\mathrm{e}(t) - F_r(t)$, respectively. Then, the desired motion behavior of the manipulator can be obtained by

$$\ddot{\xi}_p = M_v^{-1}\left(K_f \xi_f - D_v \dot{\xi}_p - K_v \xi_p\right). \tag{8}$$

Set the state as $x = [\dot{\xi}_p, \xi_p, F_e]^T$. With the assumption of $x_e = 0$, the dynamic model (7) can be written as the following nonlinear model

$$\begin{bmatrix} \ddot{\xi}_p \\ \dot{\xi}_p \\ \dot{F}_e \end{bmatrix} = \begin{bmatrix} M_v^{-1}\left(K_f(F_e - F_r) - D_v\dot{\xi}_p - K_v\xi_p\right) \\ \dot{\xi}_p \\ \mathcal{H}(x,t) \end{bmatrix}, \tag{9}$$

where $\mathcal{H}(x,t)$ is a nonlinear function related to the contact model that can be learned through machine learning methods.

The decision variable u is defined as a change of acceleration, i.e., $u = \dddot{\xi}_p$. Thus, the above formulation can be re-written as a discrete-space nominal system

$$f_{nom} = x_{t+1} = \begin{bmatrix} I & 0 & 0 \\ 0 & I & T_s \\ 0 & 0 & I \end{bmatrix} x_t + \begin{bmatrix} T_s \\ 0 \\ 0 \end{bmatrix} u_t. \tag{10}$$

IV. Controller Design

Figure 3 shows the proposed overall control scheme for robotic polishing with tool manipulation. It mainly consists of two modules to close the perception-action loop: tactile perception and interaction control. The perception module is employed to extract the tool-end interaction information inferred from the tactile feedback at the tool handle. The control module is then applied to regulate the task-oriented tool-environment interaction using the extracted information from tactile perception.

A. GPR for Tool-Environment Modeling

In contrast to problem-specific parametric models requiring manual specification, GPR stands out as a non-parametric regression approach with the potential to automatically learn latent dynamics without an explicit model. This method serves as a learning-based model suitable for diverse applications. In this work, the tool-environment dynamics is illustrated in (3),

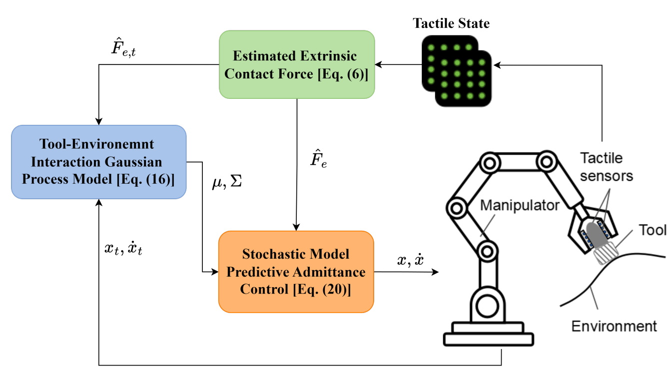

Fig. 3. The proposed control scheme diagram of tactile-guided tool-environment interaction.

where the unknown transition dynamics $\mathcal{H}(z_k)$ can be learned by GPR and system noise is $w \sim \mathcal{N}(0, \Sigma_w)$.

In the training process, the regression features z_k are selected as tuples $z_k = [x_k \ u_k]^T$ as training inputs, and the training output can be expressed as

$$y_k = g(x_k, u_k) + w_k = {B_d}^{\dagger}(x_{k+1} - f_{nom}(x_k, u_k)), \quad (11)$$

where ${B_d}^{\dagger}$ is the Moore-Penrosepseudo-inverse.

Therefore, the Gaussian process can be fully characterized as

$$g_{GP}(z) \sim \mathcal{GP}(m(z), k(z, z')), \quad (12)$$

with mean function $m(z)$ and kernel function $k(z, z')$,

$$\begin{aligned} m(z) &= \mathbb{E}[g(z)] \\ k(z, z') &= \mathbb{E}[(g(z) - m(z))(g(z') - m(z'))]. \end{aligned} \quad (13)$$

In this work, we assume a zero mean function $m(z)$ and adopt the Square Exponential Kernel as the kernel function

$$k(z, z') = \sigma_f^2 \exp\left(-\frac{1}{2}(z - z')^{\mathrm{T}} M^{-1}(z - z')\right), \quad (14)$$

where σ_f^2 is the signal variance, M denotes the diagonal matrix with characteristic length-scale.

At each time step, the states and disturbances are approximated as a Gaussian distribution $\mathcal{N}(\mu_k, \Sigma_k)$ with the state mean μ_k and variance Σ_k. To estimate the predicted state distribution across the prediction horizon, we derive linearization methods linked to the extended Kalman filter. These methods facilitate straightforward updates to the variables.

$$\begin{aligned} \mu_{k+1}^x &= f_{nom}(\mu_k^x, u_k) + B_d \mu_k^d, \\ \Sigma_{k+1}^x &= \begin{bmatrix} \nabla_x f_{nom}(\mu_k^x, u_k) & B_d \end{bmatrix} \Sigma_k \\ &\quad [\nabla_x f_{nom}(\mu_k^x, u_k) \quad B_d]^{\mathrm{T}}. \end{aligned} \quad (15)$$

By constantly adding new sensor data in real-time, the Gaussian process model is continuously being updated. Whenever new information is gathered, all the hyper-parameters of the Gaussian process are adjusted accordingly. This online learning approach ensures the model stays accurate.

B. Stochastic MPAC

The unmodeled dynamics $g(z_k)$ in (2) can be learned by GPR with the update law (15) designed above. Then, the new learning-based prediction can be formulated as:

$$x_{k+1}^x = f_{\text{nom}}(x_k^x, u_k) + B_d(g_{\mathcal{GP}}(z_k) + w), \quad (16)$$

where the process noise $w \sim \mathcal{N}(0, \Sigma^w)$.

The stochastic model can be further expressed as

$$\mu_{k+1}^x = f_{\text{nom}}(\mu_k^x, u_k) + B_d \mu_k^d. \quad (17)$$

The MPC involves solving a constrained finite horizon optimal control problem at each step. To simultaneously deal with unpredictable interactions in admittance control and different types of constraints in MPC, a novel MPAC is proposed. When there are no active constraints, MPAC should be equivalent to admittance control, that is, static feedback control. To obtain the desired behavior in (8), it is necessary to design the cost function of the MPAC problem so that it is optimally zero when the desired behavior is obtained. For this purpose, zero-valued customized cost function is defined as

$$f_o(\mu_k^x, u_k) = M_v u_k + D_v \mu_k^x(1) + K_v \mu_k^x(2) - K_f(\mu_k^x(3) - F_r). \quad (18)$$

To improve contact safety, constraints for position, velocity, and acceleration limits are formulated.

$$\mu_k^x \in \mathcal{X}, u_k \in \mathcal{U}, \quad (19)$$

Thus, the GP-based MPAC scheme is defined as follows:

$$\begin{aligned} \mu_{0:N}^{*x}, u_{0:N-1}^* = &\underset{\mu_{0:N}^{x}, u_{0:N-1}}{\arg\min} \sum_{k=1}^{N-1} f_o(\mu_k^x, u_k) + \phi(\mu_N^x) \\ &\text{s.t.} \quad \mu_0^x = \overline{x}, \quad \Sigma_0^x = 0 \\ &\qquad \mu_{k+1}^x = f_{\text{nom}}(\mu_k^x, u_k) + B_d \mu_k^d \\ &\qquad \mu_k^x \in \mathcal{X}, \\ &\qquad u_k \in \mathcal{U}, \end{aligned} \quad (20)$$

where the cost function $f_o(\mu_k^x, u_k)$ is shown with its parameter argument μ_k and decision variable u_k.

V. Experiments and Results

Several experiments have been conducted to validate the effectiveness of the proposed approach.

A. Robotic System Setup

As illustrated in Fig. 1, the robotic system setup includes a KUKA LBR iiwa 14 R820 robot arm, a Robotiq 2F-85 gripper, and two XELA 16-taxel (4×4) uSkin tactile sensors mounted on the gripper fingertips. For the polishing process, the gripper is used to grasp a polishing tool where the tactile sensors are only directly in contact with the tool's handle.

As illustrated in Fig. 4, the process of the object polishing task is divided into several steps: i) the robot grasps the tool and advances towards the surface, ii) the contact is detected by the tactile sensors, and a GP-based contact model is constructed according to the motion data, iii) the robot execute the polishing process on the contacting surface following an eight curve as the reference trajectory while maintaining a desired constant force, and iv) upon completion of the task, the robot retracts the tool away from the surface.

B. Experimental Results

The output sampling rate of the tactile sensor is 100 Hz and the control rate is 50 Hz. The impedance parameters are chosen as $M_v = 1\ \mathrm{N \cdot s^2/m}$, $D_v = 100\ \mathrm{N \cdot s/m}$, $K_v = 50\ \mathrm{N/m}$. The prediction horizon for MPC is set to 5 because the current solver has difficulty in solving the constrained QP problem for a longer horizon within the given time.

In the experiments, a repeated eight curve with a cycle time of five seconds is used as the reference motion trajectory in the x-y plane, and a constant force is set as the reference contact force. For comparison purposes, the fundamental admittance

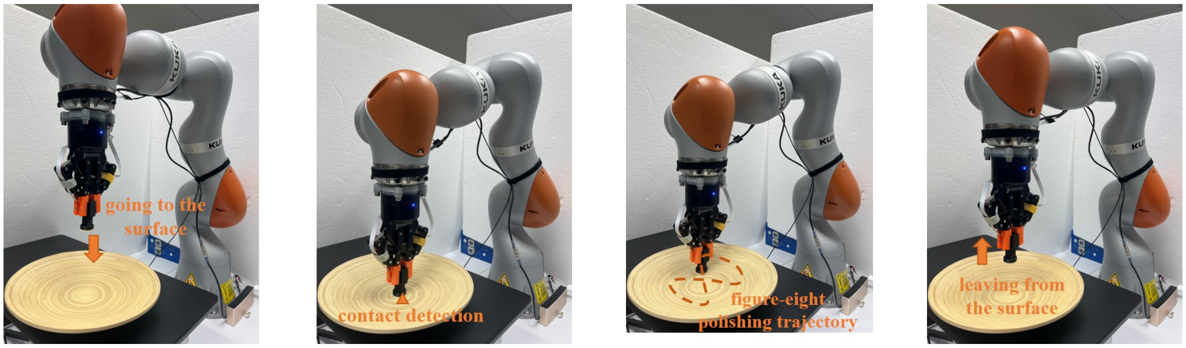

(a) (b) (c) (d)

Fig. 4. Robotic object polishing using GP-MPAC: (a) before contact; (b) contact detection; (c) polishing; (d) complete

control (AC, without the use of MPC) and the MPAC (without the use of GPR) are also applied to the robotic system set up

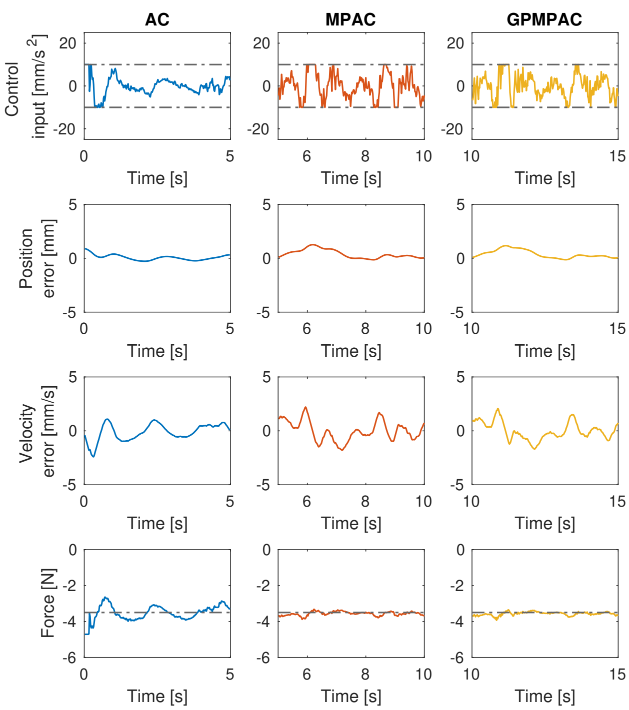

(a)

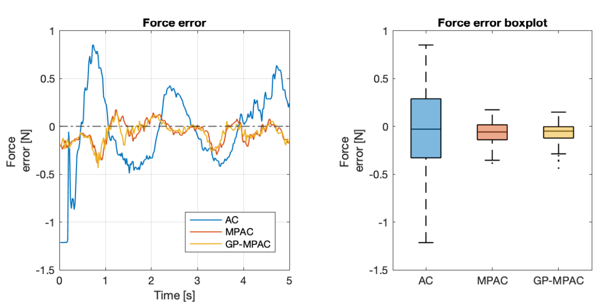

(b)

Fig. 5. Experimental results on a flat wooden surface: (a) control input, position error, velocity error and force tracking performance; (b) force error.

in the experiments.

1) Experiments on Flat Surface: In this experiment, a flat wooden surface is first used as the object to be polished. The desired force is set at -3.5 N and the experimental results using different controllers are illustrated in Fig. 5.

All three controllers can help the system regulate the tool-environmental interaction force to reach the target value. Both the MPAC and GP-MPAC perform better than the AC, which implies that the integration with MPC helps the system achieve better force control performance. Furthermore, it can be observed from the force error boxplot [see Fig. 5(b)] that the GP-MPAC can obtain slightly better force control performance than the MPAC. The root-mean-square errors (RMSEs) of using MPAC and GP-MPAC are 0.1266 N and 0.1159 N, respectively, which shows that the use of GPR can reduce the force error by about 8% for the interaction with a flat surface. Therefore, it can be concluded that more stable contact can be further achieved by integrating the GPR with MPAC.

2) Experiments on Curved Surface: To validate the performance of the proposed method in more complex environments, a curved wooden surface is used as the object to be polished in this experiment. Remarkably, the contour of the curved surface is unknown but an approximate parabola is set as the reference motion trajectory in the z-axis. The desired force is still set at -3.5 N for this wooden surface. The tracking performance of different control schemes is shown in Fig. 6.

Similar to the experiments on the flat surface, all the control schemes are still able to help the system maintain the contact force approximating the desired value. It can be also observed that the GP-MPAC achieves better force control performance than the MPAC. By comparing the force errors between both control schemes, the RMSE using MPAC is 0.1623 N while the RMSE using GP-MPAC is 0.0961 N. A significant improvement (more than 40% in terms of RMSE) can be achieved by the proposed GP-MPAC. Remarkably, the RMSEs using the proposed GP-MPAC remain at a similar level on different-shaped surfaces (i.e., flat and curved surfaces). In other words, similar force control performance can be achieved by the proposed control scheme even if the surface shape changes and there is a difference between the actual shape and the approximate reference. Therefore, it shows that the

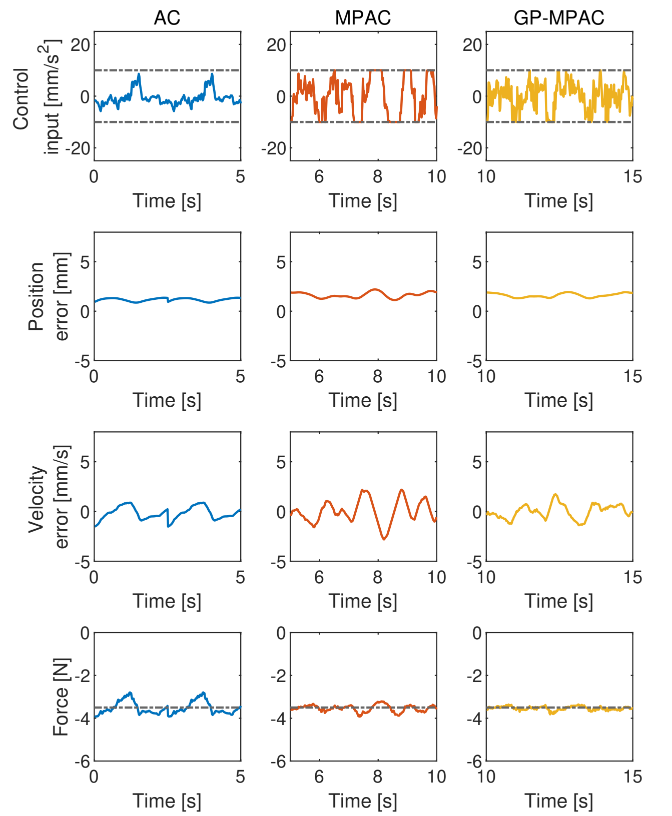

(a)

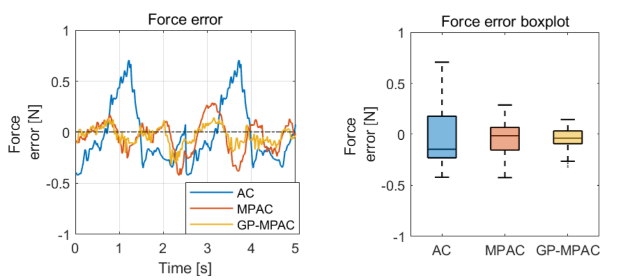

(b)

Fig. 6. Experimental results on a curved wooden surface: s(a) control input, position error, velocity error, and force tracking performance; (b) force error.

proposed control scheme demonstrates strong robustness to shape changes and uncertainties.

Besides that, the collected data (input) and the regression output of the GPR are illustrated in Fig. 7. As can be seen, the GPR can capture changes in the contact model caused by shape changes.

C. Summary

The maximum absolute error (MaxAEs) and the RMSEs of the force errors using different control schemes on different surfaces are listed in Table I, where Δ_{MPC} denotes the improvement using MPAC in comparison to AC while Δ_{GP} denotes the improvement using GP-MPAC in comparison to MPAC. The results demonstrate that the proposed GP-MPAC

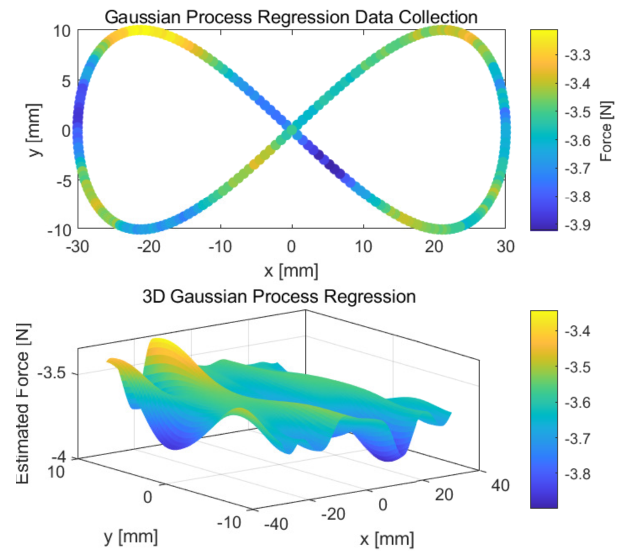

Fig. 7. The GPR estimated force experimental results.

TABLE I
RESULTS ON DIFFERENT SURFACES USING VARIOUS CONTROL SCHEMES

Error [N]	MaxAE		RMSE	
	Flat	Curve	Flat	Curve
AC	1.7863	0.7067	1.6476	0.3009
MPAC	0.3836	0.4244	0.1266	0.1623
Δ_{MPC}	78.52%	39.94%	92.35%	46.06%
GP-MPAC	0.3531	0.3210	0.1159	0.0961
Δ_{GP}	7.95%	24.38%	8.45%	40.81%

outperforms the MPAC on all surfaces, with notable enhancements observed on curved surfaces. These findings suggest that GPR significantly improves the system's adaptability to environmental variations, such as changes in shape and stiffness.

VI. Conclusion

In this paper, a Gaussian Process Model Predictive Admittance Control (GP-MPAC) method is developed for tactile-guided tool-environment interaction. Firstly, a method that integrates admittance control and model predictive admittance control, namely MPAC, is proposed to address the constraints on admittance control. Secondly, the contact force is incorporated into the state-space model of the MPAC, and GPR is employed to model the tool-environment contact force. Finally, several experiments have been performed to validate the effectiveness of the proposed control scheme. As illustrated by the results, the proposed approach achieves accurate contact force estimation and exhibits good force control performance. One future work would be to extend the proposed framework into a general form that can handle more complex tool use cases such as challenging surface cleaning.

References

[1] M. Iskandar, C. Ott, A. Albu-Schäffer, B. Siciliano, and A. Dietrich, "Hybrid Force-Impedance Control for Fast End-Effector Motions," *IEEE Robotics and Automation Letters*, vol. 8, no. 7, pp. 3931–3938, Jul. 2023.

[2] C. Seo, H. Kim, H. Jin, T. Kim, and T. Seo, "Force control of a grinding robotic manipulator with floating base via model prediction optimization control," *IEEE/ASME Transactions on Mechatronics*, vol. 28, no. 4, pp. 1911–1919, 2023.

[3] M. Dyck, A. Sachtler, J. Klodmann, and A. Albu-Schäffer, "Impedance Control on Arbitrary Surfaces for Ultrasound Scanning Using Discrete Differential Geometry," *IEEE Robotics and Automation Letters*, vol. 7, no. 3, pp. 7738–7746, Jul. 2022.

[4] Q. Ren, W. Zhu, Z. Feng, and W. Liang, "Learning-Based Force Control of a Surgical Robot for Tool-Soft Tissue Interaction," *IEEE Robotics and Automation Letters*, vol. 6, no. 4, pp. 6345–6352, Oct. 2021.

[5] P. Flores, M. Machado, M. T. Silva, and J. M. Martins, "On the continuous contact force models for soft materials in multibody dynamics," *Multibody system dynamics*, vol. 25, pp. 357–375, 2011.

[6] Z. Feng, W. Liang, J. Ling, X. Xiao, K. K. Tan, and T. H. Lee, "Precision force tracking control of a surgical device interacting with a deformable membrane," *IEEE/ASME Transactions on Mechatronics*, vol. 27, no. 6, pp. 5327–5338, 2022.

[7] P. Moreira, N. Zemiti, C. Liu, and P. Poignet, "Viscoelastic model based force control for soft tissue interaction and its application in physiological motion compensation," *Computer methods and programs in biomedicine*, vol. 116, no. 2, pp. 52–67, 2014.

[8] R. Schindeler and K. Hashtrudi-Zaad, "Online Identification of Environment Hunt–Crossley Models Using Polynomial Linearization," *IEEE Transactions on Robotics*, vol. 34, no. 2, pp. 447–458, Apr. 2018.

[9] S. Jung, T. C. Hsia, and R. G. Bonitz, "Force tracking impedance control of robot manipulators under unknown environment," *IEEE Transactions on Control Systems Technology*, vol. 12, no. 3, pp. 474–483, 2004.

[10] T. Gold, A. Völz, and K. Graichen, "Model predictive interaction control for robotic manipulation tasks," *IEEE Transactions on Robotics*, vol. 39, no. 1, pp. 76–89, 2023.

[11] M. D. Killpack, A. Kapusta, and C. C. Kemp, "Model predictive control for fast reaching in clutter," *Autonomous Robots*, vol. 40, pp. 537–560, 2016.

[12] J. Matschek, J. Bethge, P. Zometa, and R. Findeisen, "Force feedback and path following using predictive control: Concept and application to a lightweight robot," *IFAC-PapersOnLine*, vol. 50, no. 1, pp. 9827–9832, 2017.

[13] K. J. Kazim, J. Bethge, J. Matschek, and R. Findeisen, "Combined predictive path following and admittance control," in *2018 Annual American Control Conference (ACC)*. IEEE, 2018, pp. 3153–3158.

[14] A. Wahrburg and K. Listmann, "Mpc-based admittance control for robotic manipulators," in *2016 IEEE 55th Conference on Decision and Control (CDC)*. IEEE, 2016, pp. 7548–7554.

[15] M. Bednarczyk, H. Omran, and B. Bayle, "Model predictive impedance control," in *2020 IEEE International Conference on Robotics and Automation (ICRA)*, 2020, pp. 4702–4708.

[16] Z. Jin, D. Qin, A. Liu, W.-a. Zhang, and L. Yu, "Model predictive variable impedance control of manipulators for adaptive precision-compliance tradeoff," *IEEE/ASME Transactions on Mechatronics*, vol. 28, no. 2, pp. 1174–1186, 2023.

[17] R. Cao, L. Cheng, and H. Li, "Passive model predictive impedance control for safe physical human-robot interaction," *IEEE Transactions on Cognitive and Developmental Systems*, 2023.

[18] C. J. Ostafew, A. P. Schoellig, and T. D. Barfoot, "Robust constrained learning-based nmpc enabling reliable mobile robot path tracking," *The International Journal of Robotics Research*, vol. 35, no. 13, pp. 1547–1563, 2016.

[19] L. Hewing, A. Liniger, and M. N. Zeilinger, "Cautious nmpc with gaussian process dynamics for autonomous miniature race cars," in *2018 European Control Conference (ECC)*. IEEE, 2018, pp. 1341–1348.

[20] G. Torrente, E. Kaufmann, P. Föhn, and D. Scaramuzza, "Data-driven mpc for quadrotors," *IEEE Robotics and Automation Letters*, vol. 6, no. 2, pp. 3769–3776, 2021.

[21] E. Picotti, E. Mion, A. D. Libera, J. Pavlovic, A. Censi, E. Frazzoli, A. Beghi, and M. Bruschetta, "A learning-based nonlinear model predictive controller for a real go-kart based on black-box dynamics modeling through gaussian processes," *IEEE Transactions on Control Systems Technology*, vol. 31, no. 5, pp. 2055–2065, 2023.